

BABAR-CONF-02/17
SLAC-PUB-9324
July 2002

Measurement of Branching Fractions of Color-Suppressed Decays of the \bar{B}^0 Meson to $D^0\pi^0$, $D^0\eta$, and $D^0\omega$

The *BABAR* Collaboration

July 24, 2002

Abstract

We report preliminary results of an experimental investigation of the color-suppressed decays $\bar{B}^0 \rightarrow D^0\pi^0$, $D^0\eta$, and $D^0\omega$. We measure the branching fractions $\mathcal{B}(\bar{B}^0 \rightarrow D^0\pi^0) = (2.89 \pm 0.29(\text{stat.}) \pm 0.38(\text{syst.})) \times 10^{-4}$, $\mathcal{B}(\bar{B}^0 \rightarrow D^0\eta) = (2.41 \pm 0.39(\text{stat.}) \pm 0.32(\text{syst.})) \times 10^{-4}$, and $\mathcal{B}(\bar{B}^0 \rightarrow D^0\omega) = (2.48 \pm 0.40(\text{stat.}) \pm 0.32(\text{syst.})) \times 10^{-4}$. The results are based on $(48.8 \pm 0.5) \times 10^6$ $B\bar{B}$ pairs collected with the *BABAR* detector. The branching fractions of these color-suppressed decays are significantly larger than theoretical expectations based upon factorization.

Contributed to the 31st International Conference on High Energy Physics,
7/24—7/31/2002, Amsterdam, The Netherlands

Stanford Linear Accelerator Center, Stanford University, Stanford, CA 94309

Work supported in part by Department of Energy contract DE-AC03-76SF00515.

The *BABAR* Collaboration,

B. Aubert, D. Boutigny, J.-M. Gaillard, A. Hicheur, Y. Karyotakis, J. P. Lees, P. Robbe, V. Tisserand,
A. Zghiche

Laboratoire de Physique des Particules, F-74941 Annecy-le-Vieux, France

A. Palano, A. Pompili

Università di Bari, Dipartimento di Fisica and INFN, I-70126 Bari, Italy

J. C. Chen, N. D. Qi, G. Rong, P. Wang, Y. S. Zhu

Institute of High Energy Physics, Beijing 100039, China

G. Eigen, I. Ofte, B. Stugu

University of Bergen, Inst. of Physics, N-5007 Bergen, Norway

G. S. Abrams, A. W. Borgland, A. B. Breon, D. N. Brown, J. Button-Shafer, R. N. Cahn, E. Charles,
M. S. Gill, A. V. Gritsan, Y. Groysman, R. G. Jacobsen, R. W. Kadel, J. Kadyk, L. T. Kerth,
Yu. G. Kolomensky, J. F. Kral, C. LeClerc, M. E. Levi, G. Lynch, L. M. Mir, P. J. Oddone, T. J. Orimoto,
M. Pripstein, N. A. Roe, A. Romosan, M. T. Ronan, V. G. Shelkov, A. V. Telnov, W. A. Wenzel
Lawrence Berkeley National Laboratory and University of California, Berkeley, CA 94720, USA

T. J. Harrison, C. M. Hawkes, D. J. Knowles, S. W. O'Neale, R. C. Penny, A. T. Watson, N. K. Watson
University of Birmingham, Birmingham, B15 2TT, United Kingdom

T. Deppermann, K. Goetzen, H. Koch, B. Lewandowski, K. Peters, H. Schmuecker, M. Steinke
Ruhr Universität Bochum, Institut für Experimentalphysik 1, D-44780 Bochum, Germany

N. R. Barlow, W. Bhimji, J. T. Boyd, N. Chevalier, P. J. Clark, W. N. Cottingham, C. Mackay,
F. F. Wilson
University of Bristol, Bristol BS8 1TL, United Kingdom

K. Abe, C. Hearty, T. S. Mattison, J. A. McKenna, D. Thiessen
University of British Columbia, Vancouver, BC, Canada V6T 1Z1

S. Jolly, A. K. McKemey
Brunel University, Uxbridge, Middlesex UB8 3PH, United Kingdom

V. E. Blinov, A. D. Bukanin, A. R. Buzykaev, V. B. Golubev, V. N. Ivanchenko, A. A. Korol,
E. A. Kravchenko, A. P. Onuchin, S. I. Serednyakov, Yu. I. Skovpen, A. N. Yushkov
Budker Institute of Nuclear Physics, Novosibirsk 630090, Russia

D. Best, M. Chao, D. Kirkby, A. J. Lankford, M. Mandelkern, S. McMahon, D. P. Stoker
University of California at Irvine, Irvine, CA 92697, USA

C. Buchanan, S. Chun
University of California at Los Angeles, Los Angeles, CA 90024, USA

H. K. Hadavand, E. J. Hill, D. B. MacFarlane, H. Paar, S. Prell, Sh. Rahatlou, G. Raven, U. Schwanke,
V. Sharma
University of California at San Diego, La Jolla, CA 92093, USA

J. W. Berryhill, C. Campagnari, B. Dahmes, P. A. Hart, N. Kuznetsova, S. L. Levy, O. Long, A. Lu,
M. A. Mazur, J. D. Richman, W. Verkerke

University of California at Santa Barbara, Santa Barbara, CA 93106, USA

J. Beringer, A. M. Eisner, M. Grothe, C. A. Heusch, W. S. Lockman, T. Pulliam, T. Schalk, R. E. Schmitz,
B. A. Schumm, A. Seiden, M. Turri, W. Walkowiak, D. C. Williams, M. G. Wilson

University of California at Santa Cruz, Institute for Particle Physics, Santa Cruz, CA 95064, USA

E. Chen, G. P. Dubois-Felsmann, A. Dvoretskii, D. G. Hitlin, F. C. Porter, A. Ryd, A. Samuel, S. Yang
California Institute of Technology, Pasadena, CA 91125, USA

S. Jayatilleke, G. Mancinelli, B. T. Meadows, M. D. Sokoloff
University of Cincinnati, Cincinnati, OH 45221, USA

T. Barillari, P. Bloom, W. T. Ford, U. Nauenberg, A. Olivas, P. Rankin, J. Roy, J. G. Smith, W. C. van
Hoek, L. Zhang

University of Colorado, Boulder, CO 80309, USA

J. L. Harton, T. Hu, M. Krishnamurthy, A. Soffer, W. H. Toki, R. J. Wilson, J. Zhang
Colorado State University, Fort Collins, CO 80523, USA

D. Altenburg, T. Brandt, J. Brose, T. Colberg, M. Dickopp, R. S. Dubitzky, A. Hauke, E. Maly,
R. Müller-Pfefferkorn, S. Otto, K. R. Schubert, R. Schwierz, B. Spaan, L. Wilden

Technische Universität Dresden, Institut für Kern- und Teilchenphysik, D-01062 Dresden, Germany

D. Bernard, G. R. Bonneauaud, F. Brochard, J. Cohen-Tanugi, S. Ferrag, S. T'Jampens, Ch. Thiebaux,
G. Vasileiadis, M. Verderi

Ecole Polytechnique, LLR, F-91128 Palaiseau, France

A. Anjomshoaa, R. Bernet, A. Khan, D. Lavin, F. Muheim, S. Playfer, J. E. Swain, J. Tinslay
University of Edinburgh, Edinburgh EH9 3JZ, United Kingdom

M. Falbo

Elon University, Elon University, NC 27244-2010, USA

C. Borean, C. Bozzi, L. Piemontese, A. Sarti

Università di Ferrara, Dipartimento di Fisica and INFN, I-44100 Ferrara, Italy

E. Treadwell

Florida A&M University, Tallahassee, FL 32307, USA

F. Anulli,¹ R. Baldini-Ferroli, A. Calcaterra, R. de Sangro, D. Falciai, G. Finocchiaro, P. Patteri,
I. M. Peruzzi,¹ M. Piccolo, A. Zallo

Laboratori Nazionali di Frascati dell'INFN, I-00044 Frascati, Italy

S. Bagnasco, A. Buzzo, R. Contri, G. Crosetti, M. Lo Vetere, M. Macri, M. R. Monge, S. Passaggio,
F. C. Pastore, C. Patrignani, E. Robutti, A. Santroni, S. Tosi

Università di Genova, Dipartimento di Fisica and INFN, I-16146 Genova, Italy

¹ Also with Università di Perugia, I-06100 Perugia, Italy

S. Bailey, M. Morii

Harvard University, Cambridge, MA 02138, USA

R. Bartoldus, G. J. Grenier, U. Mallik

University of Iowa, Iowa City, IA 52242, USA

J. Cochran, H. B. Crawley, J. Lamsa, W. T. Meyer, E. I. Rosenberg, J. Yi

Iowa State University, Ames, IA 50011-3160, USA

M. Davier, G. Grosdidier, A. Höcker, H. M. Lacker, S. Laplace, F. Le Diberder, V. Lepeltier, A. M. Lutz,
T. C. Petersen, S. Plaszczynski, M. H. Schune, L. Tantot, S. Trincaz-Duvoid, G. Wormser

Laboratoire de l'Accélérateur Linéaire, F-91898 Orsay, France

R. M. Bionta, V. Brigljević, D. J. Lange, K. van Bibber, D. M. Wright

Lawrence Livermore National Laboratory, Livermore, CA 94550, USA

A. J. Bevan, J. R. Fry, E. Gabathuler, R. Gamet, M. George, M. Kay, D. J. Payne, R. J. Sloane,
C. Touramanis

University of Liverpool, Liverpool L69 3BX, United Kingdom

M. L. Aspinwall, D. A. Bowerman, P. D. Dauncey, U. Egede, I. Eschrich, G. W. Morton, J. A. Nash,
P. Sanders, D. Smith, G. P. Taylor

University of London, Imperial College, London, SW7 2BW, United Kingdom

J. J. Back, G. Bellodi, P. Dixon, P. F. Harrison, R. J. L. Potter, H. W. Shorthouse, P. Strother, P. B. Vidal
Queen Mary, University of London, E1 4NS, United Kingdom

G. Cowan, H. U. Flaecher, S. George, M. G. Green, A. Kurup, C. E. Marker, T. R. McMahon, S. Ricciardi,
F. Salvatore, G. Vaitsas, M. A. Winter

*University of London, Royal Holloway and Bedford New College, Egham, Surrey TW20 0EX, United
Kingdom*

D. Brown, C. L. Davis

University of Louisville, Louisville, KY 40292, USA

J. Allison, R. J. Barlow, A. C. Forti, F. Jackson, G. D. Lafferty, A. J. Lyon, N. Savvas, J. H. Weatherall,
J. C. Williams

University of Manchester, Manchester M13 9PL, United Kingdom

A. Farbin, A. Jawahery, V. Lillard, D. A. Roberts, J. R. Schieck

University of Maryland, College Park, MD 20742, USA

G. Blaylock, C. Dallapiccola, K. T. Flood, S. S. Hertzbach, R. Kofler, V. B. Koptchev, T. B. Moore,
H. Staengle, S. Willocq

University of Massachusetts, Amherst, MA 01003, USA

B. Brau, R. Cowan, G. Sciolla, F. Taylor, R. K. Yamamoto

Massachusetts Institute of Technology, Laboratory for Nuclear Science, Cambridge, MA 02139, USA

M. Milek, P. M. Patel

McGill University, Montréal, QC, Canada H3A 2T8

F. Palombo

Università di Milano, Dipartimento di Fisica and INFN, I-20133 Milano, Italy

J. M. Bauer, L. Cremaldi, V. Eschenburg, R. Kroeger, J. Reidy, D. A. Sanders, D. J. Summers

University of Mississippi, University, MS 38677, USA

C. Hast, P. Taras

Université de Montréal, Laboratoire René J. A. Lévesque, Montréal, QC, Canada H3C 3J7

H. Nicholson

Mount Holyoke College, South Hadley, MA 01075, USA

C. Cartaro, N. Cavallo, G. De Nardo, F. Fabozzi, C. Gatto, L. Lista, P. Paolucci, D. Piccolo, C. Sciacca

Università di Napoli Federico II, Dipartimento di Scienze Fisiche and INFN, I-80126, Napoli, Italy

J. M. LoSecco

University of Notre Dame, Notre Dame, IN 46556, USA

J. R. G. Alsmiller, T. A. Gabriel

Oak Ridge National Laboratory, Oak Ridge, TN 37831, USA

J. Brau, R. Frey, M. Iwasaki, C. T. Potter, N. B. Sinev, D. Strom, E. Torrence

University of Oregon, Eugene, OR 97403, USA

F. Colecchia, A. Dorigo, F. Galeazzi, M. Margoni, M. Morandin, M. Posocco, M. Rotondo, F. Simonetto,
R. Stroili, C. Voci

Università di Padova, Dipartimento di Fisica and INFN, I-35131 Padova, Italy

M. Benayoun, H. Briand, J. Chauveau, P. David, Ch. de la Vaissière, L. Del Buono, O. Hamon,
Ph. Leruste, J. Ocariz, M. Pivk, L. Roos, J. Stark

Universités Paris VI et VII, Lab de Physique Nucléaire H. E., F-75252 Paris, France

P. F. Manfredi, V. Re, V. Speziali

Università di Pavia, Dipartimento di Elettronica and INFN, I-27100 Pavia, Italy

L. Gladney, Q. H. Guo, J. Panetta

University of Pennsylvania, Philadelphia, PA 19104, USA

C. Angelini, G. Batignani, S. Bettarini, M. Bondioli, F. Bucci, G. Calderini, E. Campagna, M. Carpinelli,
F. Forti, M. A. Giorgi, A. Lusiani, G. Marchiori, F. Martinez-Vidal, M. Morganti, N. Neri, E. Paoloni,
M. Rama, G. Rizzo, F. Sandrelli, G. Triggiani, J. Walsh

Università di Pisa, Scuola Normale Superiore and INFN, I-56010 Pisa, Italy

M. Haire, D. Judd, K. Paick, L. Turnbull, D. E. Wagoner

Prairie View A&M University, Prairie View, TX 77446, USA

J. Albert, G. Cavoto,² N. Danielson, P. Elmer, C. Lu, V. Miftakov, J. Olsen, S. F. Schaffner,
A. J. S. Smith, A. Tumanov, E. W. Varnes

Princeton University, Princeton, NJ 08544, USA

² Also with Università di Roma La Sapienza, Roma, Italy

F. Bellini, D. del Re, R. Faccini,³ F. Ferrarotto, F. Ferroni, E. Leonardi, M. A. Mazzoni, S. Morganti,
G. Piredda, F. Safai Tehrani, M. Serra, C. Voena

Università di Roma La Sapienza, Dipartimento di Fisica and INFN, I-00185 Roma, Italy

S. Christ, G. Wagner, R. Waldi

Universität Rostock, D-18051 Rostock, Germany

T. Adye, N. De Groot, B. Franek, N. I. Geddes, G. P. Gopal, S. M. Xella

Rutherford Appleton Laboratory, Chilton, Didcot, Oxon, OX11 0QX, United Kingdom

R. Aleksan, S. Emery, A. Gaidot, P.-F. Giraud, G. Hamel de Monchenault, W. Kozanecki, M. Langer,
G. W. London, B. Mayer, G. Schott, B. Serfass, G. Vasseur, Ch. Yeche, M. Zito

DAPNIA, Commissariat à l'Energie Atomique/Saclay, F-91191 Gif-sur-Yvette, France

M. V. Purohit, A. W. Weidemann, F. X. Yumiceva

University of South Carolina, Columbia, SC 29208, USA

I. Adam, D. Aston, N. Berger, A. M. Boyarski, M. R. Convery, D. P. Coupal, D. Dong, J. Dorfan,
W. Dunwoodie, R. C. Field, T. Glanzman, S. J. Gowdy, E. Grauges, T. Haas, T. Hadig, V. Halyo,
T. Himel, T. Hryna, M. E. Huffer, W. R. Innes, C. P. Jessop, M. H. Kelsey, P. Kim, M. L. Kocian,
U. Langenegger, D. W. G. S. Leith, S. Luitz, V. Luth, H. L. Lynch, H. Marsiske, S. Menke, R. Messner,
D. R. Muller, C. P. O'Grady, V. E. Ozcan, A. Perazzo, M. Perl, S. Petrak, H. Quinn, B. N. Ratcliff,
S. H. Robertson, A. Roodman, A. A. Salnikov, T. Schietinger, R. H. Schindler, J. Schwiening, G. Simi,
A. Snyder, A. Soha, S. M. Spanier, J. Stelzer, D. Su, M. K. Sullivan, H. A. Tanaka, J. Va'vra,
S. R. Wagner, M. Weaver, A. J. R. Weinstein, W. J. Wisniewski, D. H. Wright, C. C. Young

Stanford Linear Accelerator Center, Stanford, CA 94309, USA

P. R. Burchat, C. H. Cheng, T. I. Meyer, C. Roat

Stanford University, Stanford, CA 94305-4060, USA

R. Henderson

TRIUMF, Vancouver, BC, Canada V6T 2A3

W. Bugg, H. Cohn

University of Tennessee, Knoxville, TN 37996, USA

J. M. Izen, I. Kitayama, X. C. Lou

University of Texas at Dallas, Richardson, TX 75083, USA

F. Bianchi, M. Bona, D. Gamba

Università di Torino, Dipartimento di Fisica Sperimentale and INFN, I-10125 Torino, Italy

L. Bosisio, G. Della Ricca, S. Dittongo, L. Lanceri, P. Poropat, L. Vitale, G. Vuagnin

Università di Trieste, Dipartimento di Fisica and INFN, I-34127 Trieste, Italy

R. S. Panvini

Vanderbilt University, Nashville, TN 37235, USA

³ Also with University of California at San Diego, La Jolla, CA 92093, USA

S. W. Banerjee, C. M. Brown, D. Fortin, P. D. Jackson, R. Kowalewski, J. M. Roney

University of Victoria, Victoria, BC, Canada V8W 3P6

H. R. Band, S. Dasu, M. Datta, A. M. Eichenbaum, H. Hu, J. R. Johnson, R. Liu, F. Di Lodovico,
A. Mohapatra, Y. Pan, R. Prepost, I. J. Scott, S. J. Sekula, J. H. von Wimmersperg-Toeller, J. Wu,
S. L. Wu, Z. Yu

University of Wisconsin, Madison, WI 53706, USA

H. Neal

Yale University, New Haven, CT 06511, USA

1 Introduction

Decays of the type $\bar{B}^0 \rightarrow D^+ h^-$ proceed through a color-allowed spectator diagram in which the W^- decays to a $\bar{u}d$ quark pair that hadronizes into the light hadron h^- . On the other hand, decays of the type $\bar{B}^0 \rightarrow D^0 h^0$ proceed through a color-suppressed spectator diagram that requires color matching of the quark and the antiquark from the W^- with the c and \bar{d} quarks. Since perturbative calculations of hadronic B decay rates are not possible, we must rely on models for predictions. The naive factorization model predicts very low branching fractions for color-suppressed decays, in the range $0.3\text{--}0.7 \times 10^{-4}$ [1, 2]. However, this model is supported by HQET only for color-allowed decays, while color-suppressed decays receive substantial corrections [3] that depend upon the decay mode. Experimental measurements of the branching fractions of color-suppressed B decays provide an important test of theoretical models and can be used to improve the models.

In this paper we report on the observation of the three color-suppressed decays $\bar{B}^0 \rightarrow D^0\pi^0$, $\bar{B}^0 \rightarrow D^0\eta$, and $\bar{B}^0 \rightarrow D^0\omega$. The \bar{B}^0 decay into $D^0\pi^0$ has been observed previously by the CLEO Collaboration [4], all three decays have been observed by the Belle Collaboration [5].

2 The *BABAR* detector and dataset

The data used in this analysis were collected with the *BABAR* detector at the PEP-II asymmetric e^+e^- storage ring at the $\Upsilon(4S)$ resonance, between October 1999 and December 2001. This data sample contains $(48.8 \pm 0.5) \times 10^6$ $B^0\bar{B}^0$ and B^+B^- pairs.

The *BABAR* detector is described in detail elsewhere [6]. We briefly summarize the detector systems most relevant to this analysis. The *BABAR* detector contains a 5-layer silicon vertex tracker (SVT) and a 40-layer drift chamber (DCH) situated in a 1.5 T solenoidal magnetic field. These devices detect charged particles and measure their momentum and ionization energy loss (dE/dx). Surrounding the DCH are fused-silica quartz bars of a ring-imaging Cherenkov detector (DIRC). This detector measures the Cherenkov angle of light generated in the bars. The charged particle identification (PID) combines the dE/dx measurements of the SVT, DCH, and DIRC. Photons are detected in a CsI(Tl) crystal electromagnetic calorimeter (EMC). The EMC detects photons with energies as low as 20 MeV.

The interactions of particles traversing the detector are simulated using the GEANT4 [7] program. Beam-induced backgrounds are taken into account. Signal and generic background Monte Carlo samples are used to study the effect of the event selection criteria and to estimate the backgrounds. The generic background Monte Carlo simulation consists of $e^+e^- \rightarrow q\bar{q}$ ($q = u, d, s, c$) and B^+B^- and $B^0\bar{B}^0$ events.

3 Analysis method

Here, we describe the reconstruction and the selection of the three color-suppressed modes $\bar{B}^0 \rightarrow D^0\pi^0$, $\bar{B}^0 \rightarrow D^0\eta$, and $\bar{B}^0 \rightarrow D^0\omega$.

3.1 Particle selection

Photons are identified by energy deposits in contiguous crystals in the EMC. They must have an energy greater than 30 MeV and a lateral shower shape compatible with electromagnetic showers. Charged particle tracks (except those used to reconstruct ρ mesons) must have at least 12 hits in the

DCH and $p_t > 100 \text{ MeV}/c$. Tracks must extrapolate to within 20 mm of the e^+e^- interaction point in the plane transverse to the beam axis and within 50 mm along the beam axis. Charged kaon candidates are identified using a likelihood function that combines dE/dx and DIRC information. The likelihood function is used to define a tight kaon criterion and a loose criterion to veto pions. To satisfy the tight kaon criteria, the track must also have $p_t > 250 \text{ MeV}/c$ and an angle with the beam between 0.45 and 2.5 rad so that the candidate is within the fiducial region of the DIRC.

3.2 Light hadron and D meson reconstruction

The neutral π^0 and η mesons are reconstructed from photon pairs. Mass constrained fits are applied to π^0 and η candidates. The photons used to reconstruct the η must have energies greater than 200 MeV. Any photon used to reconstruct an η candidate is vetoed if it can be paired with an additional photon with energy greater than 150 MeV to form a π^0 candidate with mass in the range 120 - 150 MeV/c^2 . This reduces the contribution from the $B^- \rightarrow D^{(*)0}\rho^-$ background when a photon from a high energy π^0 from ρ decay is associated with another photon to form an η candidate. This veto also reduces the cross-feed from color-suppressed $D^{(*)0}\pi^0$ modes to the $D^0\eta$ channel.

Candidate ω mesons are reconstructed from $\pi^+\pi^0\pi^-$ candidates with a vertex constraint applied to the $\pi^+\pi^-$. To reduce combinatoric background, the charged pion candidates must have a momentum greater than 200 MeV/c while the π^0 must have an energy greater than 250 MeV.

The D^0 mesons are reconstructed in three decay modes: $K^-\pi^+$, $K^-\pi^+\pi^0$, and $K^-\pi^+\pi^+\pi^-$. Vertex constraints are applied to the charged particles and mass constraints are applied using all particles. In the $K^-\pi^+$ final state the kaon candidate must satisfy the pion veto requirement while in the $K^-\pi^+\pi^0$ and $K^-\pi^+\pi^+\pi^-$ final states the kaon candidate must satisfy the tight kaon criterion because of the increased background present in these combinations. All pion candidates must fail the tight kaon criterion. To reduce combinatoric background in the $K^-\pi^+\pi^0$ final state, we require in addition that either the $\pi^-\pi^0$ or one of the two $K^-\pi$ combinations have an invariant mass consistent with an intermediate resonant state ρ^- or K^* . The energy of the π^0 is also required to be greater than 300 MeV.

The \bar{B}^0 mesons are reconstructed from D^0h^0 ($h^0 = \pi^0, \eta, \omega$) pairs. For the final state $D^0\omega$ we apply a vertex constraint to the D^0 and the two charged pions. The energy and momentum of the \bar{B}^0 are calculated from the improved energies and momenta of the D^0 and h^0 that result from the vertex and mass fits.

The $\bar{B}^0 \rightarrow D^0\pi^0$ sample is contaminated by the color-allowed $B^- \rightarrow D^0\rho^-$ decay that has a branching fraction about fifty times larger than the color-suppressed decay. The contamination is caused by asymmetric $\rho^- \rightarrow \pi^-\pi^0$ decays where the π^0 has most of the energy of the ρ^- . The decay channel $B^- \rightarrow D^0\rho^-$ is reconstructed and $\bar{B}^0 \rightarrow D^0\pi^0$ candidates that are also reconstructed as $B^- \rightarrow D^0\rho^-$ are vetoed. To make this veto as efficient as possible, the ρ^- is reconstructed using not only pion candidates as defined above but also low momentum pion candidates that are reconstructed using the SVT alone. The veto reduces the signal efficiency by 10%. Other channels vetoed are $\bar{B}^0 \rightarrow D^{*0}h^0$. D^{*0} candidates are reconstructed from a D^0 paired with either a π^0 with momentum less than 300 MeV/c in the e^+e^- center-of-mass frame or with a photon. In the latter case, the photon must not be a partner in a pair of photons forming a π^0 candidate. The $D^{*0} - D^0$ mass difference is required to be less than 2.0 standard deviations away from its nominal value.

The reconstructed masses of the D^0 , π^0 , and η are required to be within $\pm 2.5\sigma$ of their nominal value [8]. The D^0 mass resolutions are about 6, 12, and 5 MeV/c^2 for the $K^-\pi^+$, $K^-\pi^+\pi^0$, and $K^-\pi^+\pi^+\pi^-$ decay modes, respectively, while the π^0 and η mass resolutions are about 8 and

$16 \text{ MeV}/c^2$, respectively. The reconstructed mass of the ω candidates is required to be within $\pm 25 \text{ MeV}/c^2$ of the ω nominal value [8].

3.3 B candidate selection

Both b and u, d, s , and c quark-antiquark production contribute combinatoric background events for which the mass of the candidate B does not peak near the nominal B mass. To reject the u, d, s , and c components, we apply several selection criteria based upon the shape of the event in the e^+e^- center-of-mass frame.

The ratio of the second to the zeroth Fox-Wolfram moment [9] must be $R_2 < 0.6$. For each reconstructed \bar{B}^0 candidate, we compute the thrust and sphericity axes of both the candidate and the rest of the event [10], and we apply a selection on the angles θ_{thr} and θ_{sph} between the two axes, respectively. The distributions of $|\cos \theta_{\text{thr}}|$ and $|\cos \theta_{\text{sph}}|$ peak near 1.0 for $udsc$ background while they are nearly flat for B decays. Thus we require $|\cos \theta_{\text{sph}}| < 0.85$ and $|\cos \theta_{\text{thr}}| < 0.85$ for the $D^0\pi^0$ and the $D^0\eta$ final states. For the $D^0\eta$ final state we take advantage of $\sin^2 \theta^*$ distribution of the production angle θ^* of the B mesons in the e^+e^- center of mass system, demanding $|\cos \theta^*| < 0.80$. The corresponding distribution is almost flat for any kind of combinatoric background. For the $D^0\omega$ channel, as the ω is a polarized vector particle, we use two other angles. The first angle is θ_N , defined as the angle between the normal to the plane of the three daughter pions in the ω center-of-mass frame and the ω direction in the B center-of-mass frame. The second angle is θ_D , the angle between one of the three pions in the ω center-of-mass frame and the direction of one of the two remaining pions in the center-of-mass frame of these two pions. The signal events are distributed as $\cos^2 \theta_N$ and $\sin^2 \theta_D$, while the corresponding distributions are flat for combinatoric background. We select only events inside a region of the three-dimensional parameter space of the angles θ^*, θ_N , and θ_D with high signal population.

In a small fraction of the events, even after the selection criteria and after the veto of $B^- \rightarrow D^0\rho^-$ (for $D^0\pi^0$) or $\bar{B}^0 \rightarrow D^{*0}h^0$ (for $D^0\eta/\omega$), more than one B candidate survives. We select the candidate with the lowest value of

$$\chi_B^2 = \left(\frac{m_D - m_D^{\text{nom}}}{\sigma_{m_D}} \right)^2 + \left(\frac{m_h - m_h^{\text{nom}}}{\sigma_{m_h}} \right)^2,$$

where σ_{m_D} and σ_{m_h} are the average mass resolutions of the D^0 and the light hadron h^0 . The D^0 mass resolution depends on the D^0 decay mode. The ratios in parentheses are found to be approximately Gaussian with mean values near 0.0 and standard deviations near 1.0.

4 Event yields

The energy-substituted mass is defined as $m_{\text{ES}} = \sqrt{(E_B^*)^2 - (p_B^*)^2}$ and the energy difference is defined as $\Delta E = E_D^* + E_h^* - E_B^*$. Here p_B^* is the measured momentum of the B candidate and E_D^* and E_h^* are the energies of the D^0 and the h^0 , all calculated from the measured D^0 and h^0 momenta. E_B^* is the beam energy (and thus the energy of the B meson). All quantities with a * are calculated in the e^+e^- center-of-mass frame. Signal events have $m_{\text{ES}} \approx m_B = 5.279 \text{ GeV}/c^2$ and $\Delta E \approx 0$. The m_{ES} resolution is dominated by the beam energy spread and is approximately $3 \text{ MeV}/c^2$, independent of the B decay mode. The ΔE resolutions for the $D^0\pi^0$ and $D^0\eta$ modes are dominated by the photon energy resolution in the EMC for the π^0 or η decay products. They

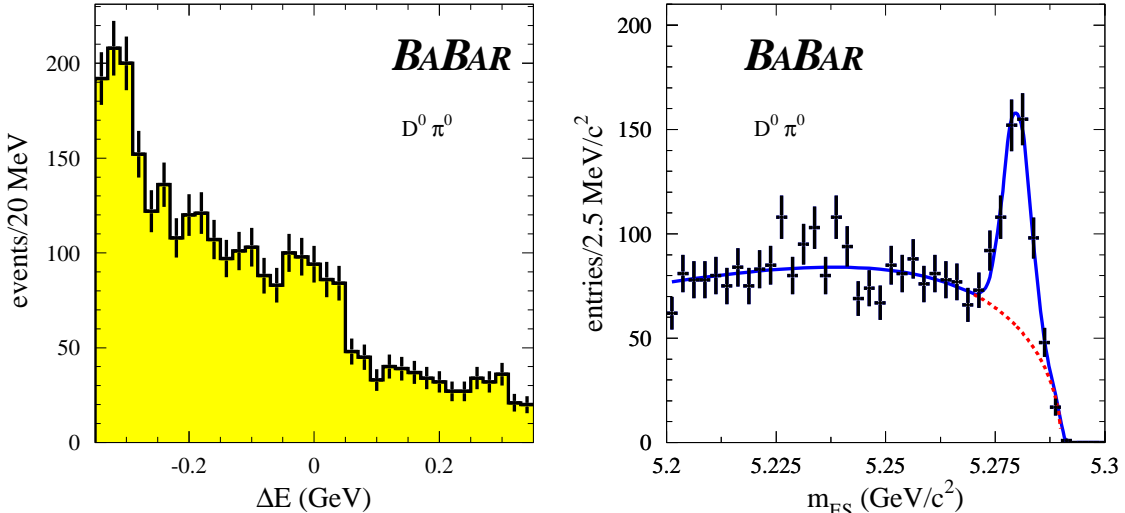


Figure 1: Distributions of ΔE (left, with m_{ES} in the range $5.27\text{--}5.29\text{ GeV}/c^2$) and beam energy substituted mass m_{ES} (right, with $-90 < \Delta E < 100\text{ MeV}$) for $\bar{B}^0 \rightarrow D^0\pi^0$ candidates.

are approximately $30 - 40$ MeV. The ΔE resolution is better for the $D^0\omega$ mode because it is dominated by tracking resolution and is approximately 20 MeV.

The m_{ES} distributions with a selection on ΔE and the ΔE distributions with a selection on m_{ES} for $D^0\pi^0$, $D^0\eta$, and $D^0\omega$ are shown in Figs. 1, 2, and 3, respectively. The m_{ES} distributions are shown for $-90 < \Delta E < 100\text{ MeV}$ for $D^0\pi^0$, $|\Delta E| < 90\text{ MeV}$ for $D^0\eta$, and $|\Delta E| < 60\text{ MeV}$ for the $D^0\omega$ final states, respectively. The ΔE distributions are shown for m_{ES} in the range $5.27\text{--}5.29\text{ GeV}/c^2$. We observe clear signals in all three channels.

We perform a least-squares fit of a function consisting of the sum of a Gaussian and an Argus background function [11] to the m_{ES} distribution for the $D^0\pi^0$ final state. For the $D^0\eta$ and $D^0\omega$ modes, where the signal yields are lower, we perform an unbinned maximum likelihood fit of the same functions to the m_{ES} distribution. The Argus function accounts for random combinatoric background originating from both $udsc$ continuum, τ leptons, two-photon processes, and $B\bar{B}$ events but not for “peaking background”. The peaking background accounts for specific channels described by a Gaussian very similar to the real signal.

We investigate peaking background by studying a generic background $B\bar{B}$ Monte Carlo sample. The only significant peaking background in the $\bar{B}^0 \rightarrow D^0\pi^0$ selection originates from $B^- \rightarrow D^{(*)0}\rho^-$ with an undetected low-momentum π^- . According to the Monte Carlo simulation, the veto described in Sec. 3.2 rejects 75% of $B^- \rightarrow D^{(*)0}\rho^-$ events in the range $\Delta E < -90\text{ MeV}$ but only 16% of that background in the signal range $-90 < \Delta E < 100\text{ MeV}$. The veto thus causes a flattening of the background in the ΔE distribution thereby reducing the systematic error from the uncertainty in the energy resolution of the EMC. The peaking background is a smaller problem for $D^0\eta$ and $D^0\omega$ modes and contributes less than 12% of the total background in the signal region. We use the generic $B\bar{B}$ Monte Carlo sample to estimate the amount of peaking background. Uncertainty in the branching fraction is included as a systematic error.

For the $D^0\pi^0$ final state, the least-squares fit to the m_{ES} distribution in Fig. 1 gives the un-

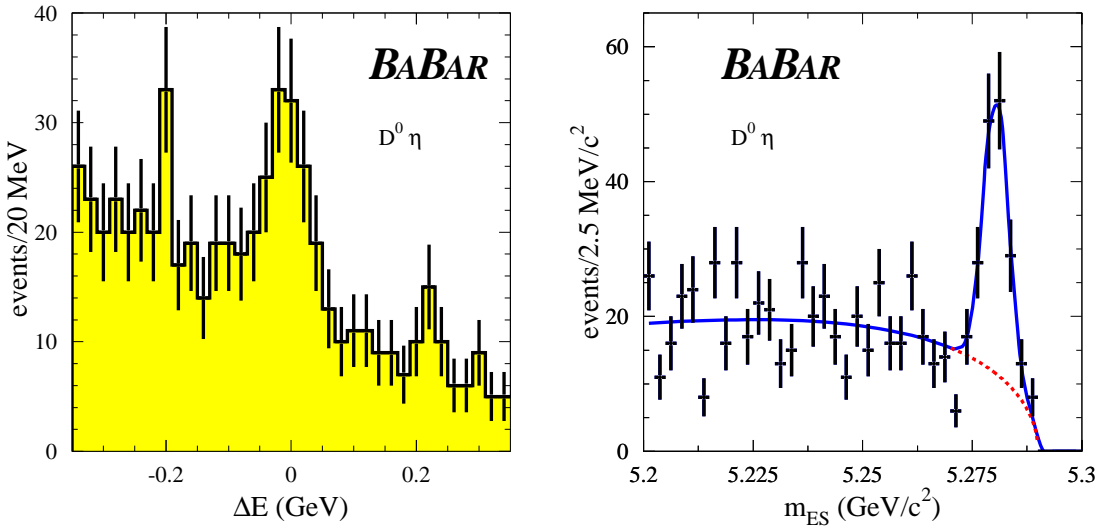


Figure 2: Distributions of ΔE (left, with m_{ES} in the range $5.27\text{--}5.29\text{ GeV}/c^2$) and beam energy substituted mass m_{ES} (right, with $|\Delta E| < 90\text{ MeV}$) for $\bar{B}^0 \rightarrow D^0 \eta$ candidates.

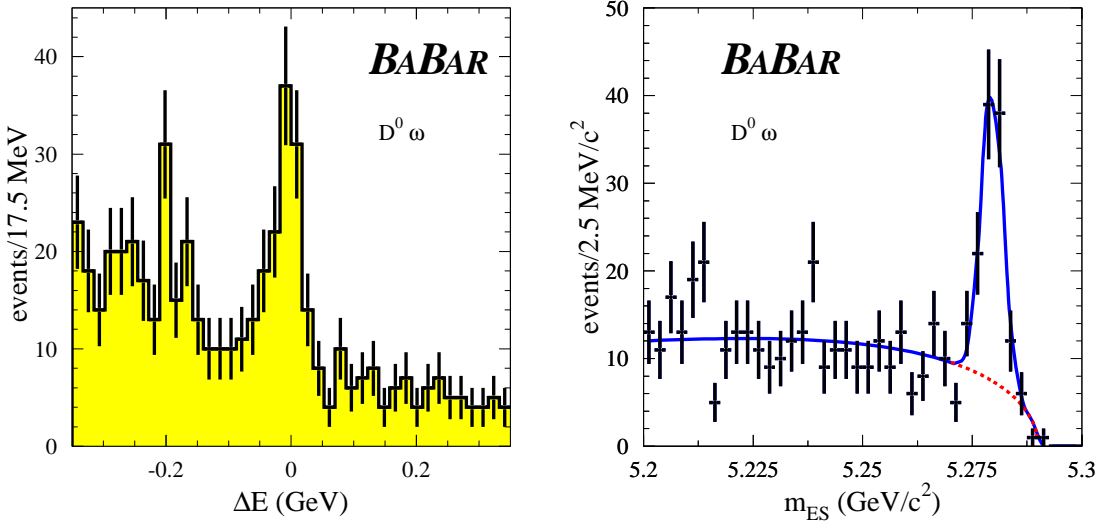


Figure 3: Distributions of ΔE (left, with m_{ES} in the range $5.27\text{--}5.29\text{ GeV}/c^2$) and beam energy substituted mass m_{ES} (right, with $|\Delta E| < 60\text{ MeV}$) for $\bar{B}^0 \rightarrow D^0 \omega$ candidates.

corrected event yield as the area under the Gaussian. The $D^0\eta$ and $D^0\omega$ modes have smaller signal yields so the contribution parametrized by the Argus function is subtracted from the event yield obtained from the number of entries in the signal region defined by $5.27 < m_{\text{ES}} < 5.29$ and $|\Delta E| < 90 \text{ MeV}$ for $D^0\eta$ and $|\Delta E| < 60 \text{ MeV}$ for the $D^0\omega$ final states. Finally, after subtraction of the estimated peaking background we obtain the signal yield. We obtain 291 ± 31 , 101 ± 14 , and 78 ± 12 for the $D^0\pi^0$, $D^0\eta$ and $D^0\omega$ final states, respectively, see Table 1.

Event yields must be corrected for cross-feed from other color suppressed modes. Cross-feed to each signal from $\bar{B}^0 \rightarrow D^{(*)0}h^0$ decays is investigated using the branching fractions measured by the CLEO [4] and Belle [5] Collaborations for the $D^{*0}h^0$ final states. For each h^0 the dominant contribution to $\bar{B}^0 \rightarrow D^0h^0$ arises from the associated $B^0 \rightarrow D^{*0}h^0$ modes. In the signal region, we estimate that the event yields for the $D^0\pi^0$, $D^0\eta$, and $D^0\omega$ final states receive contributions equal to 4.5%, 8.3%, and 2.4% from cross-feed.

The acceptance \mathcal{A} , as determined from signal Monte Carlo samples, must be corrected for differences between data and Monte Carlo simulation in tracking, vertex fitting, and particle identification. We correct the Monte Carlo simulation results using the outcome of detailed studies of detector performances in which control sets of data are compared with their Monte Carlo simulation. These procedures provide corrections that are applied per track (for track reconstruction efficiency), per kaon candidate (for particle identification efficiency), and per vertex fit (for vertex fit efficiency).

Dividing corrected signal yields (\mathcal{S}) by the number of $B\bar{B}$ events in the data sample $N(B\bar{B})$, the corrected acceptances (\mathcal{A}), and the secondary branching fractions of the D^0 and the h^0 into the reconstructed final states X and Y respectively, gives branching fractions as

$$\mathcal{B}(\bar{B}^0 \rightarrow D^0h^0) = \frac{\mathcal{S}}{N(B\bar{B}) \times \mathcal{A} \times \mathcal{B}(D^0 \rightarrow X) \times \mathcal{B}(h^0 \rightarrow Y)}.$$

The resulting branching fractions and their statistical errors are listed in Table 1.

5 Systematic uncertainties and results

Systematic errors are associated with the corrections discussed above. In addition, we have considered systematic errors from other sources. Uncertainties in the acceptances from photon detection account for imperfect simulation of photon energy and position resolution, thus affecting π^0 and η reconstruction and the ΔE resolution. We have also investigated uncertainties in the simulation of peaking and combinatoric background. For the $D^0\pi^0$ mode the systematic error associated with the veto of the $B^- \rightarrow D^0\rho^-$ background has been studied and is part of the systematic error on the background estimate. We have varied the selection criteria described in Sec. 3.1 and 3.3 in order to assign a systematic error to the event selection. The errors from the counting of $B\bar{B}$ pairs, from the branching fractions of D^0 and h^0 secondary decays [8], and the statistical error from the Monte Carlo samples used to determine the signal acceptance have also been evaluated. Table 2 summarizes these systematic errors for the three final states $D^0\pi^0$, $D^0\eta$, and $D^0\omega$.

We obtain the branching fractions $\mathcal{B}(\bar{B}^0 \rightarrow D^0\pi^0) = (2.89 \pm 0.29(\text{stat.}) \pm 0.38(\text{syst.})) \times 10^{-4}$, $\mathcal{B}(\bar{B}^0 \rightarrow D^0\eta) = (2.41 \pm 0.39(\text{stat.}) \pm 0.32(\text{syst.})) \times 10^{-4}$, and $\mathcal{B}(\bar{B}^0 \rightarrow D^0\omega) = (2.48 \pm 0.40(\text{stat.}) \pm 0.32(\text{syst.})) \times 10^{-4}$. They are listed in Table 1. These results are preliminary. The branching fractions are in good agreement with previous results from the CLEO [4] and Belle [5] Collaborations. They are more precise mainly due to larger sample of B decays. The branching fractions are considerably larger than the factorization predictions for these three modes.

Table 1: Signal event yields, $\mathcal{A} \times \mathcal{B}(D^0 \rightarrow X) \times \mathcal{B}(h^0 \rightarrow Y)$, and preliminary $\mathcal{B}(\bar{B}^0 \rightarrow D^0 h^0)$. The signal event yields shown are not corrected for cross-feed.

B^0 decay	Event yield	$\mathcal{A} \times \mathcal{B}(D^0 \rightarrow X) \times \mathcal{B}(h^0 \rightarrow Y)$ (%)	$\mathcal{B}(\bar{B}^0 \rightarrow D^0 h^0)(10^{-4})$
$D^0\pi^0$	291 ± 31	2.1	$2.89 \pm 0.29(\text{stat.}) \pm 0.38(\text{syst.})$
$D^0\eta$	101 ± 14	0.9	$2.41 \pm 0.39(\text{stat.}) \pm 0.32(\text{syst.})$
$D^0\omega$	78 ± 12	0.6	$2.48 \pm 0.40(\text{stat.}) \pm 0.32(\text{syst.})$

Table 2: Fractional systematic errors on the measured branching fractions.

Category	$D^0\pi^0$ (%)	$D^0\eta$ (%)	$D^0\omega$ (%)
Tracking	2.1	2.0	3.6
Vertex fit	1.4	1.4	2.5
Kaon identification	2.5	2.5	2.5
Cross feed	2.3	4.3	1.2
γ, π^0 , and η detection	5.3	3.6	6.0
ΔE resolution	5.7	6.7	4.6
Background estimate	4.4	3.2	5.2
Event selection	7.8	7.6	5.3
Number of $B\bar{B}$ pairs	1.1	1.1	1.1
$\mathcal{B}(D^0)$ and $\mathcal{B}(h^0)$	4.2	4.5	4.5
Monte Carlo statistics	0.7	1.5	2.4
Total	13.3	13.5	12.9

6 Acknowledgments

We are grateful for the extraordinary contributions of our PEP-II colleagues in achieving the excellent luminosity and machine conditions that have made this work possible. The success of this project also relies critically on the expertise and dedication of the computing organizations that support *BABAR*. The collaborating institutions wish to thank SLAC for its support and the kind hospitality extended to them. This work is supported by the US Department of Energy and National Science Foundation, the Natural Sciences and Engineering Research Council (Canada), Institute of High Energy Physics (China), the Commissariat à l’Energie Atomique and Institut National de Physique Nucléaire et de Physique des Particules (France), the Bundesministerium für Bildung und Forschung and Deutsche Forschungsgemeinschaft (Germany), the Istituto Nazionale di Fisica Nucleare (Italy), the Research Council of Norway, the Ministry of Science and Technology of the Russian Federation, and the Particle Physics and Astronomy Research Council (United Kingdom). Individuals have received support from the A. P. Sloan Foundation, the Research Corporation, and the Alexander von Humboldt Foundation.

References

[1] M. Neubert and B. Stech, “Non-Leptonic in *Heavy Flavours II*”, eds. A.J. Buras and M. Lindner, World Scientific, Singapore, 1998.

- [2] A. Deandrea and A.D. Polosa, Eur. Phys. J. C **22**, 677 (2002).
- [3] M. Neubert and A.A. Petrov, Phys. Lett. B **519**, 50 (2001).
- [4] The CLEO Collaboration, T.E. Coan *et al.*, Phys. Rev. Lett. **88**, 062001 (2002).
- [5] The Belle Collaboration, K. Abe *et al.*, Phys. Rev. Lett. **88**, 052002 (2002).
- [6] The *BABAR* Collaboration, B. Aubert *et al.*, Nucl. Instr. Meth. **479**, 1 (2002).
- [7] The Geant4 Collaboration, CERN preprint CERN-IT-2002-003, submitted to Nucl. Instr. Meth.
- [8] Particle Data Group, K. Hagiwara *et al.*, Phys. Rev. D **66**, 010001 (2002).
- [9] G.C. Fox and S. Wolfram, Phys. Rev. Lett. **41**, 1581 (1978).
- [10] The *BABAR* Physics Book, The *BABAR* Collaboration, eds. P.F. Harrison and H.R. Quinn, SLAC-R-504 (October 1998).
- [11] The ARGUS Collaboration, H. Albrecht *et al.*, Phys. Lett. B **185**, 218 (1987); **241**, 278 (1990).